

Scale effects or sampling bias?

N. Barton

NGI, Oslo, Norway

ABSTRACT: A wide range of scale effects and potential scale effects in rock engineering are reviewed. These include uniaxial compression strength, joint roughness and shear strength, conductivity-shear coupling, shear stiffness, failure modes, and stress-strain behaviour. Sampling bias and sampling disturbance effects may be responsible for incorrect conclusions concerning some of the apparent scale effects.

1 INTRODUCTION

Numerous potential scale effects are evident in rock mechanics. Many are real effects, but many are undoubtedly caused by the difficulties in obtaining representative samples. Large samples are more easily damaged and may therefore demonstrate lower strength or stiffness since the larger sampling size tends to include more "flaws", a fundamental scale effect would of course be expected; however, it may be exaggerated out of proportion by the sampling preparation, extraction or testing process. In this paper a fairly wide ranging look will be taken at many of the areas where scale effects are expected or suspected. The author's personal experiences lend support to many of the interesting observations made by authors to this workshop on Scale Effects in Rock Masses.

2 THE DILEMMA OF STRESS EFFECTS

It may be wise to start this review by pointing out one scale effect problem which may never be resolved, before going on to more tangible problems which have been explained or show potential for being explained.

Compilation of direct shear test data for rock joints tested under low stress levels, show very large variations in shear strength, while compilations of high stress triaxial data for faulted rock specimens show relatively small variations in

shear strength. An equally wide range of rock types may have been tested in each case.

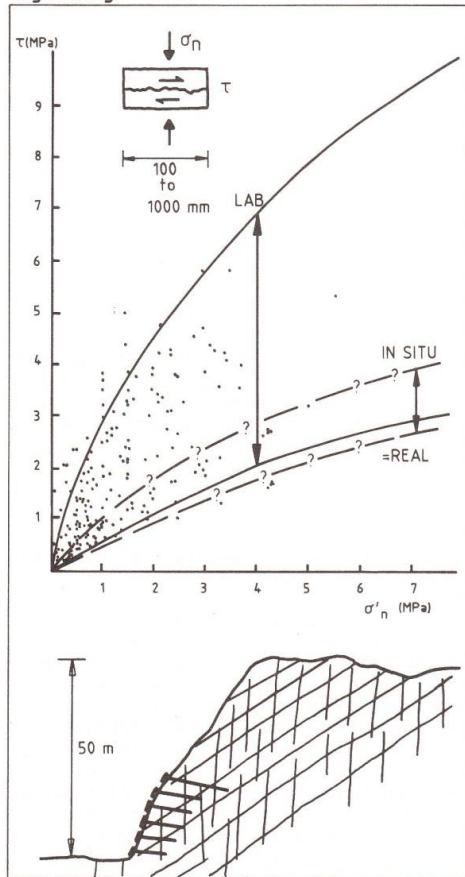
Figure 1 illustrates these different ranges of shear strength. It also illustrates the approximate ratio of test sizes: small-finger-size cylinders may represent apparatus test limits when measuring the triaxial shear strength of "faulted rock" specimens at normal stress levels in the kilobar range of stresses. This reduced specimen size is not showing a reversed scale effect. It is the enormous stress that is removing the effects of variable rock strength and discontinuity roughness, otherwise seen in tests on discontinuities in rock.

The stippled envelopes shown in Figure 1 indicate the potential scale effect for rock joints at low (engineering) stress levels. The scale effect at kilobar stress levels can only be inferred from geotectonics; but it is presumably much less marked than the scale effect we as rock engineers must live with in engineering design.

3 SCALE EFFECT ON UNIAXIAL COMPRESSION STRENGTH

This fundamental index of rock strength has been the subject of numerous scale effect investigations over the last 30 to 40 years. A useful compilation of data is that given by Lama and Gonano (1976),

Engineering



Crustal

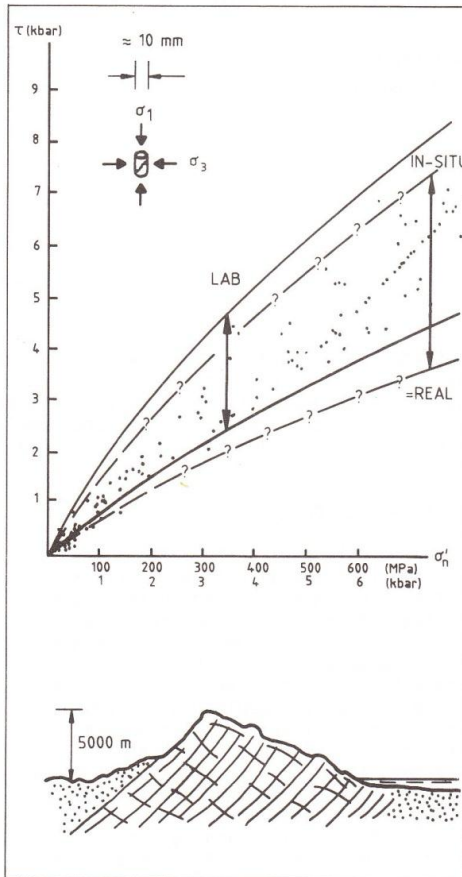


Figure 1. Different magnitudes of scale effect are expected under high and low stress. Adapted from Barton (1976). Additional data from Byerlee (1978).

which is reproduced in Figure 2.

Hoek and Brown's (1980) empirical equation for the unconfined compression strength of 10 mm to 200 mm diameter laboratory specimens has been successfully extrapolated by South African workers (see Wagner, 1987) for application to fracturing in excavations in massive quartzites of 2 and 3 metres in span. Based on the experimental curve shown in Figure 3, and Hoek and Brown's equation, a logical simplification would be:

$$\sigma_c = \sigma_{c50} (50/d)^{0.2} \quad (1)$$

where

σ_{c50} = unconfined compression strength of 50 mm specimens
 d = specimen diameter (mm)

This equation will later be compared with scaling rules used for extrapolating the shear strength of rock joints. It will also be of interest to compare the data for 63 mm and 194 mm samples of Lac du Bonnet granite reported by Jackson and Lau (1990) in this workshop, with the above equation.

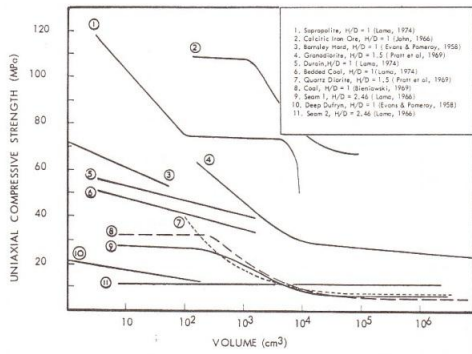


Figure 2. Scale effect on uniaxial strength, after Lama and Gonano (1976).

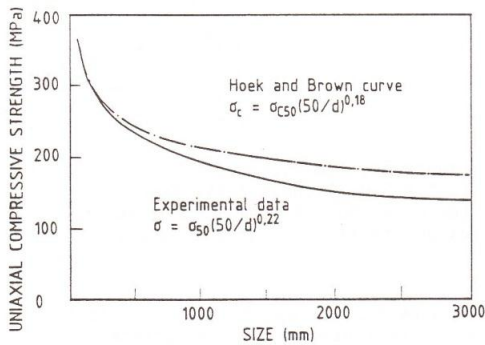


Figure 3. Empirical equations for scale effect on uniaxial strength, after Hoek and Brown (1980) and Wagner (1987).

4 THE SURFACE GEOMETRY SCALE EFFECT

It is undoubtedly true that discontinuities in rock can exhibit both higher and lower shear strength when size is increased. Large scale undulations may become relevant in slope design, which could not be sampled in laboratory samples, or in in-situ tests. Small steps in a joint caused by cross jointing would tend to be avoided in any sampling programme, likewise intact portions between joints ("intact bridges"). If we ignore these complicating, but very real components of strength, and concentrate our attention on continuous joints sampled at different scale, some fundamental and well known results are evident.

Figure 4 illustrates two classic representations of joint roughness by Patton (1966) and Fecker and Rengers (1971), and an illustrative application of the

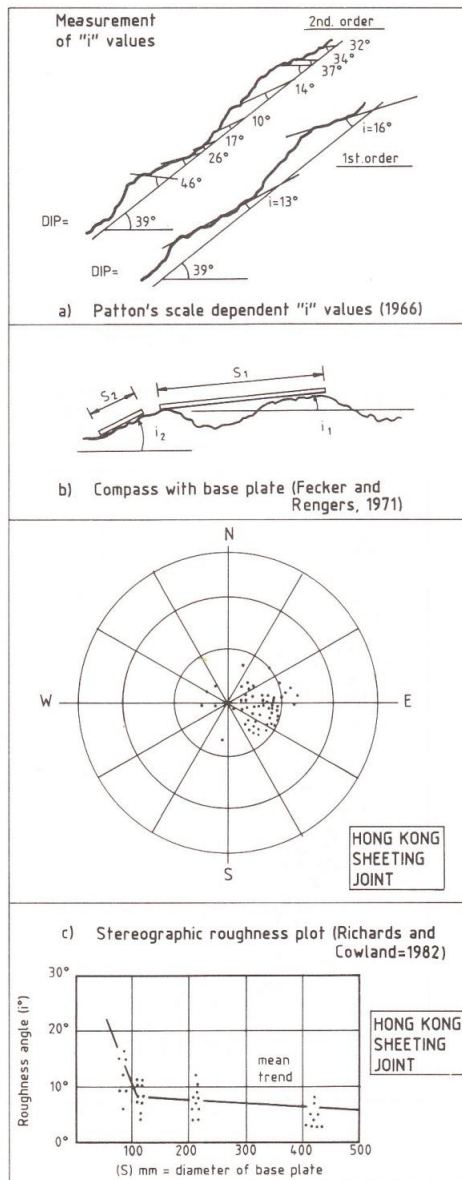


Figure 4. Measurement of (i) values in the field, after Patton (1966), Fecker and Rengers (1971) and Richards and Cowland (1982).

compass-with-base-plate method by Richards and Cowland (1982). The mean trend of reducing (i) values with sampling length

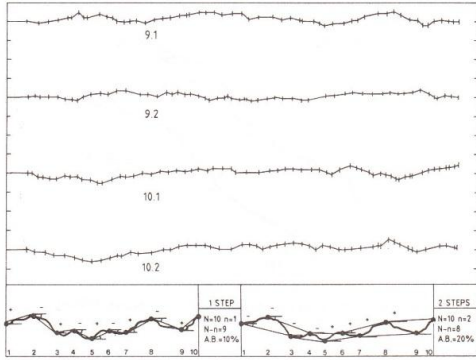


Figure 5a. Computational analysis of (i) values at different scale, Barton (1971).

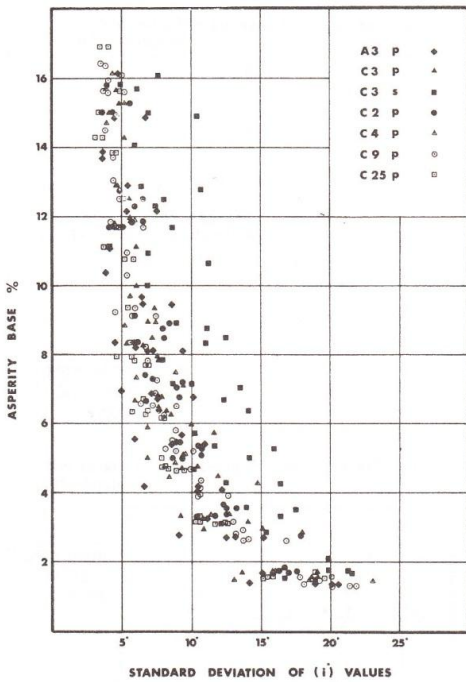


Figure 5b. Results from statistical analysis of roughness for seven types of fracture surface including stepped (■). Barton (1971).

is expected, and in many ways is similar to small scale measurements of the same phenomena, as reported by Barton (1971). Figure 5a illustrates computer drawn

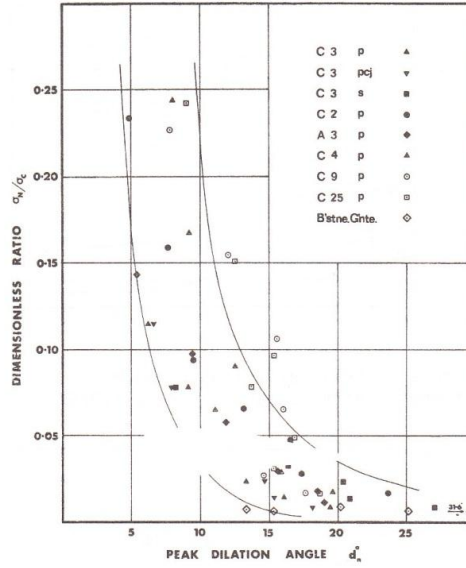


Figure 5c. Analogous behaviour of dilation ($d_n^0 \approx S.D.i$) and stress/strength ratio ($\sigma_n/\sigma_c \times 100 \approx 2 \times AB\%$) compared with (i) value statistics, Barton (1971).

roughness profiles of stereographically measured tension fracture surfaces in various model materials. "Sampling" of roughness with different "asperity base" lengths produces a consistently reducing (i) value as scale is increased. The plot of asperity base (%) versus the standard deviation of (i) values (Figure 5b) shows remarkable similarity to a plot of the peak dilation angles measured over a range of stress to strength (σ_n/σ_c) ratios for the same samples.

The standard deviation of the (i) values is the position on a histogram for a particular asperity base, such that 67% of the observations lie below the S.D.(i) value, and 33% above it. Viewed as a shearing analogy, the 33% of observations of steeper (i) values are "sheared" through, while the 67% of shallower angles remain "unsheared".

The angle S.D(i) $^\circ$ and the asperity base length A.B.% represent only the up-slope of an imaginary controlling "asperity", which just remains unsheared at the normal stress simulated. By doubling this base length the whole controlling "asperity" is simulated. In other words asperity base (A.B.%) is really a misnomer since, as calculated, it is only half a real

asperity base. It can be concluded from Figure 5 (b,c) that the following are useful approximations for relating roughness with the peak dilation angle (d_n) under a given stress to strength ratio.

1. $(\sigma_n / \sigma_c \cdot 100 (\%)) = 2 \cdot \text{A.B.}(\%)$
2. $d_n = \text{S.D.}(i)^\circ$ (2)

We should of course note the fact that the uniaxial strength may itself reduce with increasing asperity size, as discussed later.

It is interesting to note the work reported by Maerz and Franklin (1990) to this workshop, concerning roughness scale effect and fractal dimension. Their results also showed an apparent increase in roughness with decreasing baselength, based on "shadow profilometry" of a 5 m long joint surface. Their roughness profile was determined not to be a fractal object, and a roughness scale effect was therefore confirmed.

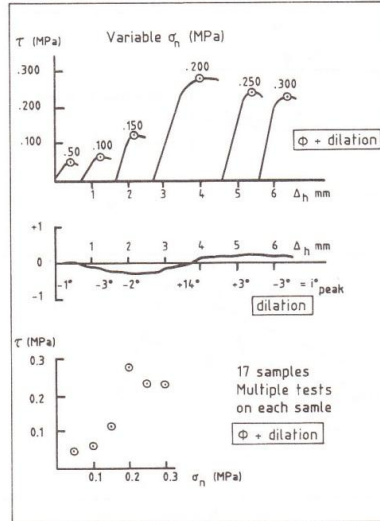
The reducing (i) value with increased sampling length shown in Figure 4 does not solve the problem of shear strength input for slope stability, even if it was possible to claim that (i) = 8° was representative. The remaining unknown is the basic frictional strength that should be added to this (i) value.

Hencher and Richards (1982 and 1989) approach this problem by performing multistage shear tests on joints recovered in drill core, and making careful measurements of the dilation (or contraction) at each stage of a test. Their procedure is illustrated in Figure 6.

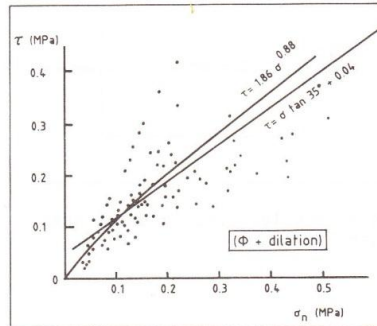
The dilation-corrected multi-stage tests suggest that an angle of 40° can be added to the above (i) value of 8° in the particular case of sheeting joints in Hong Kong granites.

At first sight this approach appears sound. It is easy to imagine that the corrected ϕ value (= 40°) is higher than the usual basic friction angle (ϕ_b) for planar surfaces in granite (about 30°) due to the component of asperity strength that is not corrected for when subtracting the dilation angle. The problem is caused by scale effect on this asperity strength component. Bandis et al. (1981) demonstrated that the asperity strength component could fall by as much as 8° in progressing from 60 mm to 360 mm test samples.

Figure 7(a) illustrates the classic Newland and Allely (1957) equation for sliding up an inclined plane, and the (i) value dilemma (Figure 7b) faced by all



Uncorrected multistage test



Uncorrected multistage tests

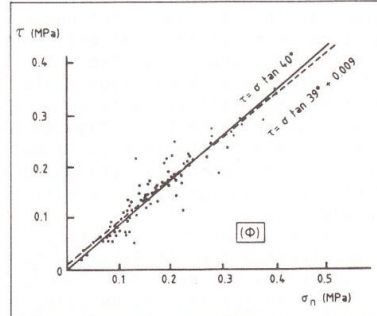


Figure 6. Correction of multi-stage shear test data using measured dilations, after Hencher and Richards (1982, 1989).

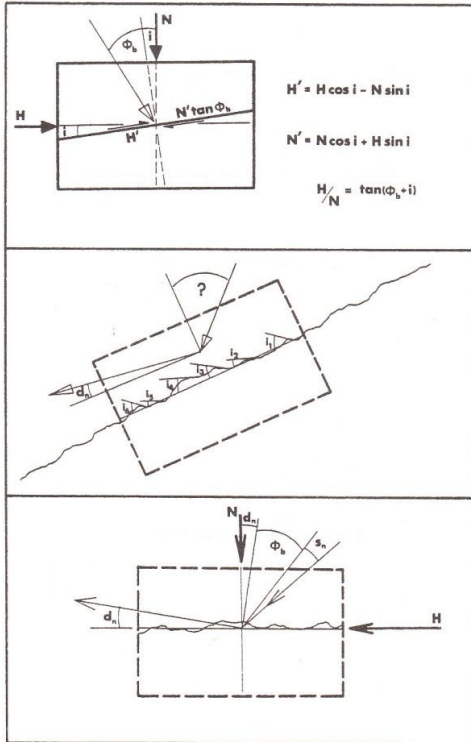


Figure 7. Angular components of shear strength (Barton, 1971).

rock slope engineers. The three basic angular components of shear strength are illustrated in Figure 7(c). The upper block dilates at a peak dilation angle (d_n) that may have little relation to any of the (i) values. The total angular component also contains the term S_n (asperity failure component) which is strongly scale dependent for rough surfaces, as will be shown again later.

It is unlikely that the laboratory dilation-corrected "basic" friction angle of 40° derived by Hencher and Richards (1982, 1989) can justifiably be added to an estimated field-scale (i) value of 8° to obtain a field design value of 48° . Of course the in situ value may well be this high due to the steps and rock bridge problems referred to earlier; it may also be lower than 48° unless effective normal stress levels are unusually low.

5 AN ALTERNATIVE APPROACH TO SHEAR STRENGTH ESTIMATION AT DIFFERENT SCALES

An alternative to the $\phi+i$ approach to rock joint shear strength and scale effect allowance is the JRC, JCS empirical method developed by Barton and Choubey (1977) and later refined by Barton and Bandis (1982). In this approach:

$$"\phi+i" = JRC_0 \log \left[\frac{JCS_0}{\sigma_n} \right] + \phi_r \quad (3)$$

The roughness term $(JRC)_0$ and the logarithmic strength/stress ratio represent a stress- and roughness-dependent (i) value. A further improvement to this (i) value estimation was the introduction of size-dependent JRC and JCS values, termed JRC_n and JCS_n .

Roughness profiles representing 100 mm long joint surfaces and corresponding measured JRC_0 values are reproduced from Barton and Choubey (1977) in Figure 8.

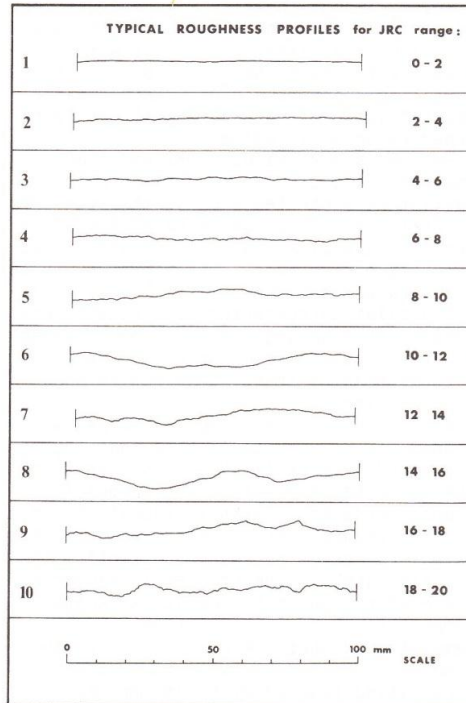


Figure 8. Joint roughness coefficient (JRC_0) and corresponding surface roughness profiles at 100 mm scale. Barton and Choubey (1977).

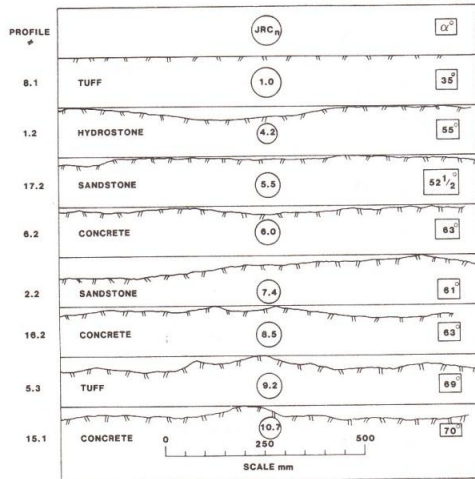


Figure 9. Joint roughness coefficient (JRC_n) and corresponding surface roughness profiles at 1000 mm scale. Bakhtar and Barton (1984).

Corresponding results for much larger surfaces are reproduced in Figure 9. A reduction in the value of JRC is obviously apparent at the larger scale, and the tilt angles required to attain shear failure along these surfaces is also noticeably less than that measured in tilt tests on the roughest laboratory-size samples, which may exceed 80°.

Tilt tests as illustrated at two different scales in Figure 10 cannot be utilized unless drill core or sufficient joint sets are available to release jointed blocks. An alternative, and rather crude approach to roughness measurement is illustrated in Figure 11. Reducing JRC with increased sample length is usual, but may of course be reversed if steps or large scale waviness are significant factors in the local joint geometry.

The method of peak shear strength estimation favoured by the author is the utilization of reduced JRC and JCS values to allow for the natural block size within the rockmass of interest. The reduction coefficients for JRC_n/JRC₀ and JCS_n/JCS₀ derived by Bandis et al. (1981) from tests on rock joints and model joint replicas are reproduced in Figure 12. Full scale strength can be estimated from the following equation:

$$\phi' = JRC_n \log \left[\frac{JCS_n}{\sigma'} \right] + \phi_r + i \quad (4)$$

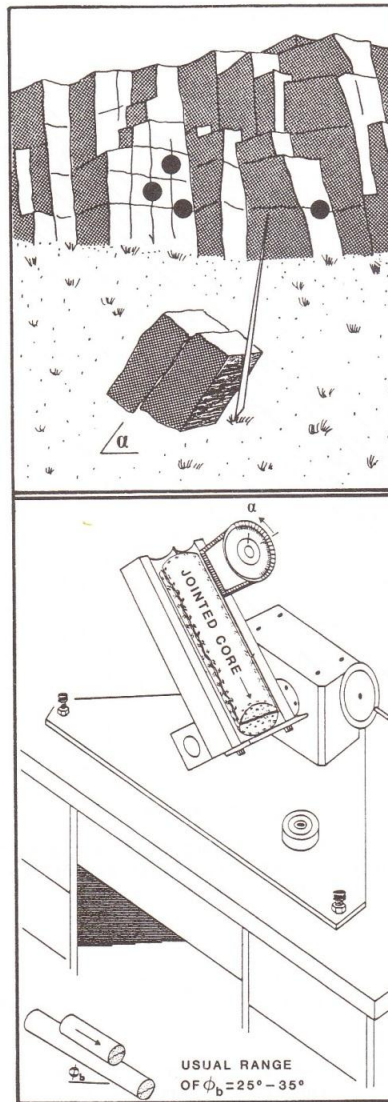


Figure 10. Tilt tests for measuring JRC at laboratory and field scale.

Where i = large scale waviness not sampled at natural block size. Approximate equations for estimating JRC_n and JCS_n at larger scale are as follows:

$$JRC_n \approx JRC_0 \left[\frac{L_n}{L_0} \right]^{-0.02} JRC_0 \quad (5)$$

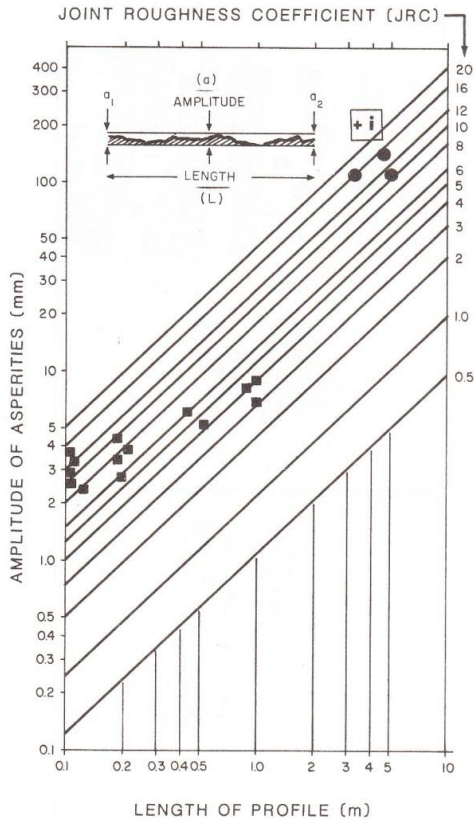


Figure 11. Roughness amplitude measurement at different scales for first approximation of the JRC value.

$$JCS_n \approx JCS_0 \left[\frac{L_n}{L_0} \right]^{-0.03} JRC_0 \quad (6)$$

where L_0 = laboratory size joint samples (nominal 100 mm)
 L_n = natural block size

It is of interest to compare equation 6 representing the empirically observed reduction in joint wall compression strength ("asperity strength") with equation 1 for uniaxial compressive strength. The forms of the two equations, which were derived quite independently, are almost identical:

$$(\sigma_c)_n = (\sigma_c)_0 \left[\frac{d}{50} \right]^{-0.2} \quad (7)$$

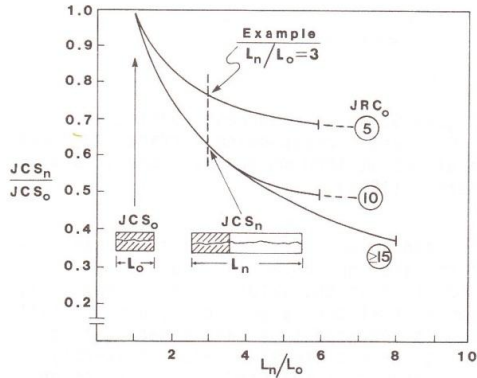
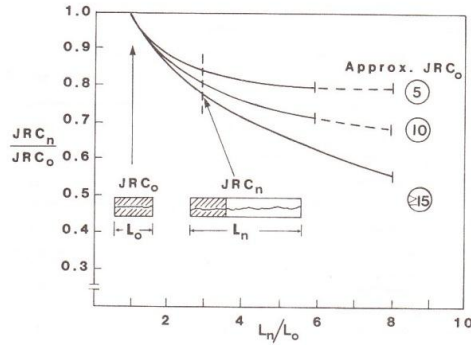


Figure 12. Method of estimating JRC_n and JCS_n values for larger sizes of rock joint, based on laboratory-size values (JRC_0 and JCS_0) after Bandis et al. (1981).

An analysis of the consequences of incorrect allowance for scale effects in shear strength estimation is given in Figure 13. the relative error (%) is defined as:

$$\frac{\tau(\text{peak})[\text{actual} \pm \text{error}] - \tau(\text{peak})[\text{actual}]}{\tau(\text{peak})[\text{actual}]} \times 100\%$$

It is apparent that roughness is of dominating importance at lower stress levels, while ϕ_r (which is assumed not to be scale dependent) is of great importance at higher stress levels. These observations are apparently consistent with the schematic diagrams of scale effects at low and high stress given in Figure 1.

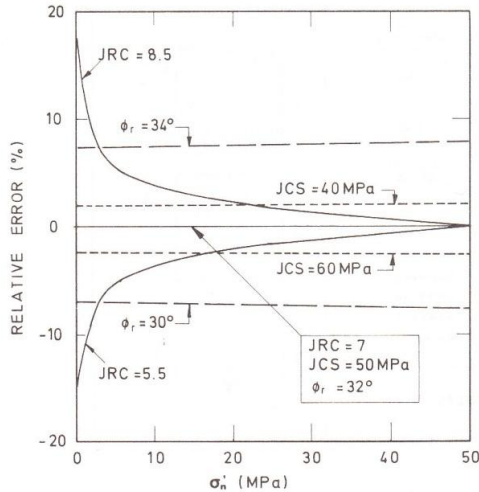


Figure 13. Consequences of parameter errors or scale effect errors in estimating shear strength. Barton (1980).

6 EFFECT OF BLOCK SIZE ON STRENGTH AND DEFORMABILITY

It is extremely difficult to perform realistic three-dimensional testing of rockmasses to evaluate the real effects of the test size or block size. However, simplified tests can be performed which help to clarify certain aspects of behaviour.

A very basic test shown in Figure 14 demonstrates quite convincingly that block size effects JRC. The measured tilt angle of 59° for the large jointed slab of granite represents a JRC value of 5.5, compared to 8.8 for the mean tilt angle of 69° for the eighteen small joint samples sawn from the same slab.

Figure 15 demonstrates even greater differences when an assembly of small blocks is tilted en masse. The latter were joint replicas fabricated with the same batch of model material and cast against the same joint surface.

Presumably the increased degree of freedom for small block rotations allows the smaller, steeper asperities to be properly "sampled", as compared to the poorer degree of "sampling" achieved by a large, stiff monolithic block.

The next logical step in a block size investigation, following the above simple cases, is the shearing of an assembly of blocks of different sizes. Figure 16 shows schematically the approximate effect

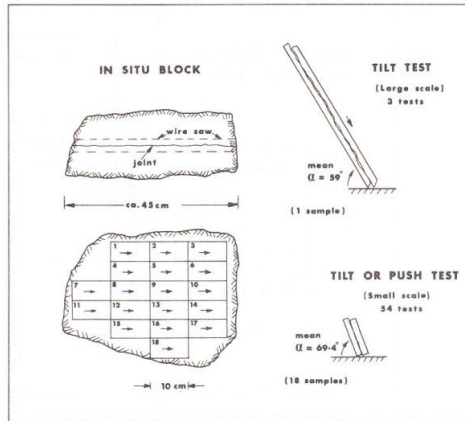


Figure 14. Scale effect on tilt angle caused by block size. Single block tests (Barton and Choubey 1977).

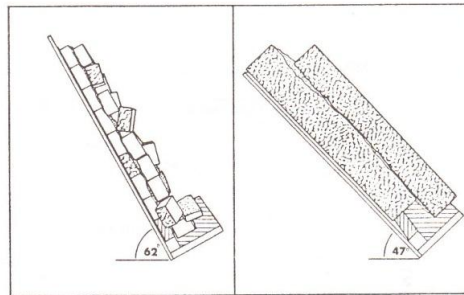


Figure 15. Scale effect on tilt angle caused by block size. Bandis et al. (1981).

of individual block size on the shear strength of the jointed mass. Biaxial samples consisting of 4000, 1000 and 250 blocks were created in the same model material using a double-bladed guillotine device.

Measured shear stress ($\sigma_1 - \sigma_3$) - strain behaviour in major principal (ϵ_1) and minor principal (ϵ_2) strain directions are shown in Figure 17. Local translational shear failure occurred at lower differential stress level in the assembly with larger blocks. The assemblies with smallest blocks always failed in rotation, in the manner of kink band formation. This failure mode did not however, occur until higher differential stresses were reached, i.e. the heavily jointed assembly had higher shear resistance than the more massive "rock masses".

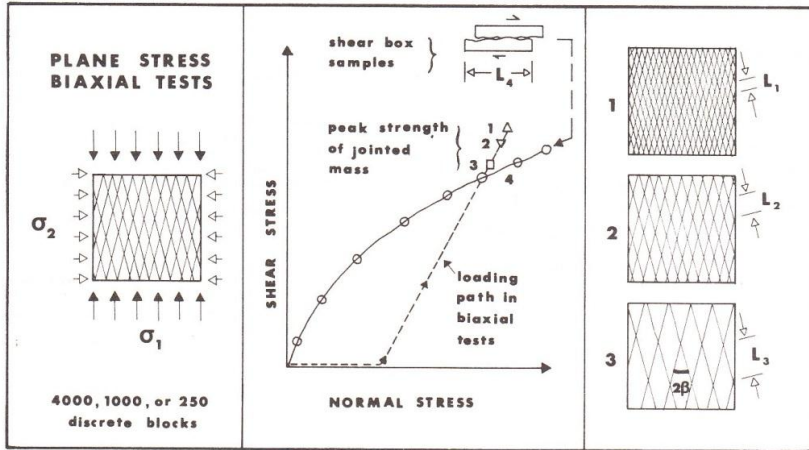


Figure 16. Effect of individual block size on the shear strength of an assembly of blocks. Barton and Hansteen (1979).

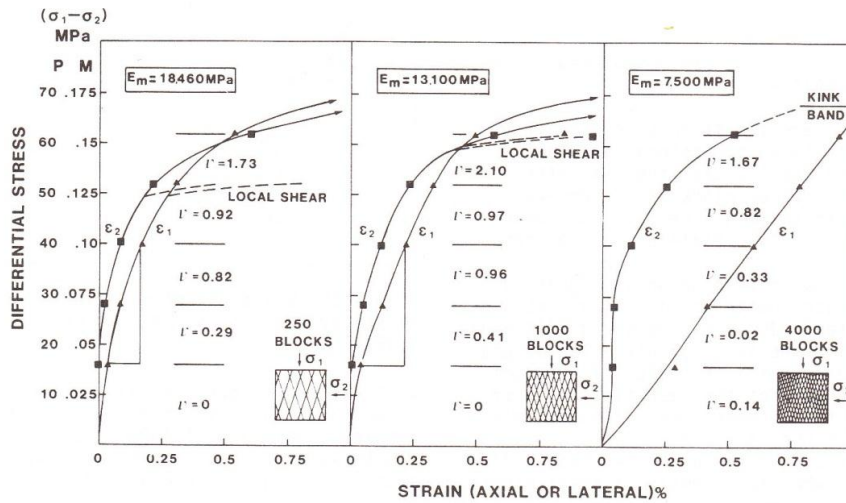


Figure 17. Stress-strain behaviour of jointed assemblies of blocks.

As expected the latter had great stiffness. Deformation moduli, when converted to prototype scale, were 18.5, 13.1 and 7.5 GPa respectively for the largest intermediate and smallest block sizes. Very large mass "Poisson ratios" were recorded as compared to intact rock, due to the joint shears, dilations and rotations that were occurring.

It is of considerable interest to compare the different shapes of the stress-strain curves. The assemblies with large and intermediate sized blocks showed classic concave shape, signifying joint shear as the dominant mode. The assembly of smallest blocks showed virtually linear stress-strain behaviour all the way up to failure.

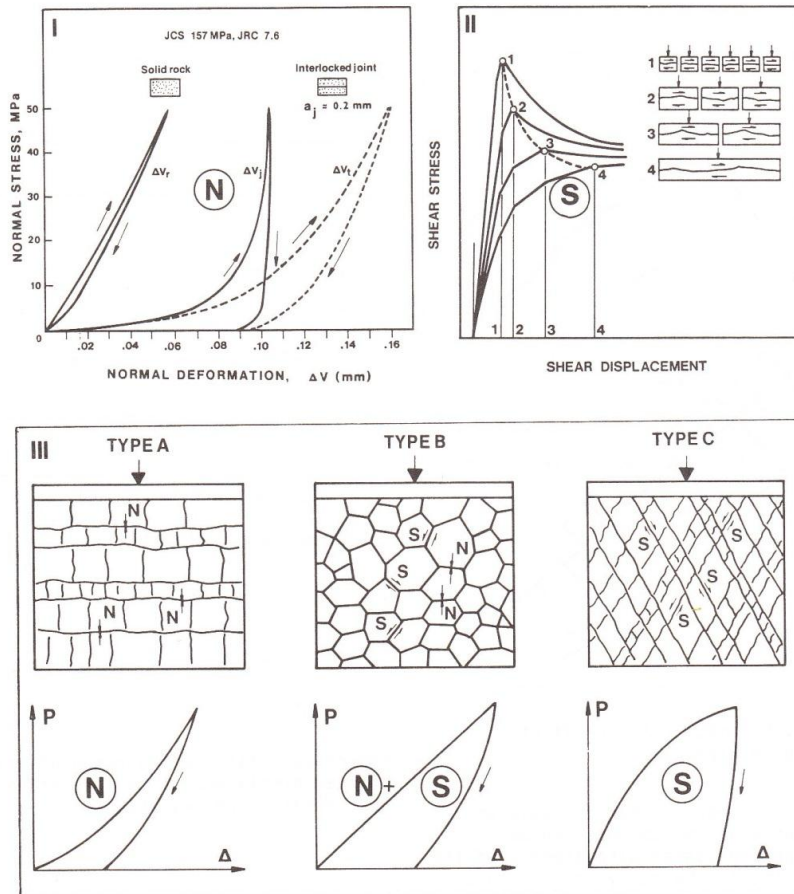


Figure 18. Normal (N) and shear (S) components of joint deformation determine the general form of stress-strain curves for loading tests on rock masses. Barton (1986), Bandis et al. (1981, 1983).

Potential explanations for the various forms of load-deformation curves registered in large scale loading tests of rock masses are given in Figure 18. They relate to the shape of individual joint closure (N) and joint shear (S) components.

An interesting question arises when trying to understand the linear stress-strain behaviour of the heavily jointed assembly (Figure 17, 4000 blocks). Is this because of type 1 (small block) shear behaviour (see Figure 18 II), or is it because of combined shearing (S) and closure (N) when so many blocks are loaded simultaneously?

7 SCALE EFFECTS ON PEAK SHEAR DISPLACEMENT

Figure 19 is a highly schematic exaggerated drawing of the effect of block size on the displacement needed to reach peak shear strength in jointed rock masses. An assembly of some 600 direct shear test data points indicate the wide variation of the ratio δ/L for various discontinuity classes.

Histograms of the same data (Figure 20) when divided into three groups of test size (30 - 300 mm, 300 mm - 3 m, 3 m - 12 m) indicate log-normal type distributions in general. The "tails" may

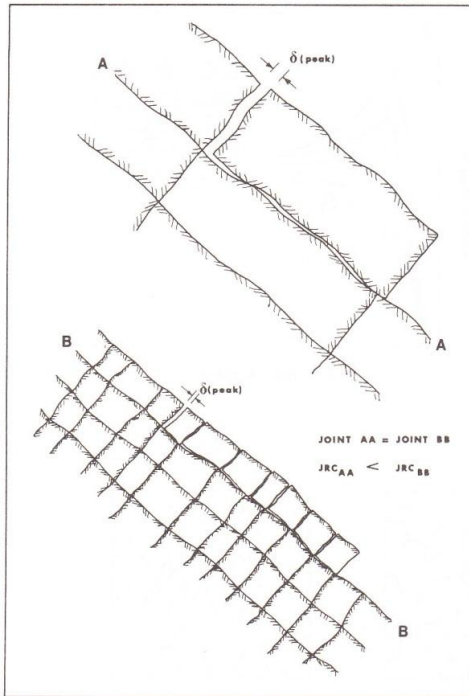


Figure 19. Schematic of the effect of block size on $\delta(\text{peak})$.

be caused by poorly located displacement measurement instrumentation. In many cases, the true shear displacement of the discontinuity is obviously smaller than that measured.

Figure 21 illustrates the apparent consistency in displacements observed in shear tests that involve loading in shear, and earthquake slip magnitudes which involve unloading in shear. An analysis of the data indicates that the following equation gives a reasonable approximation to the observed values:

$$\delta = \frac{L}{500} \left[\frac{\text{JRC}}{L} \right]^{0.33} \quad (8)$$

where δ = slip magnitude required to mobilize peak strength, or that occurring during unloading in an earthquake

L = length of joint or faulted block (meters)

JRC = joint roughness coefficient (>0)

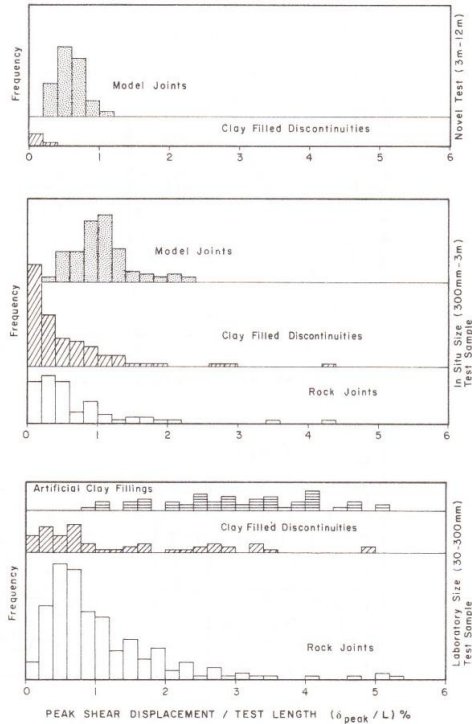


Figure 20. Histograms showing distribution of peak displacements as a function of test lengths and test types.

- Example 1. Laboratory Specimen
 Assume: JRC = 15 (rough)
 $L = 0.1 \text{ m}$
 Equation 8 gives $\delta = 1.0 \text{ mm}$
- Example 2. Natural Jointed Block
 Assume: JRC = 7.5
 $L = 1.0 \text{ m}$
 Equation 8 gives $\delta = 3.9 \text{ mm}$
- Example 3. Earthquake Fault
 Assume: JRC = 0.5 \approx residual
 $L = 100 \text{ km}$
 Equation 8 gives $\delta = 3.6 \text{ m}$

The above examples of size effects illustrate that equation 4 gives an acceptable degree of accuracy for most practical applications. The implication that (δ) is smaller when surfaces are smoother or closer to residual (JRC \approx 0) also appears to be consistent with observations.

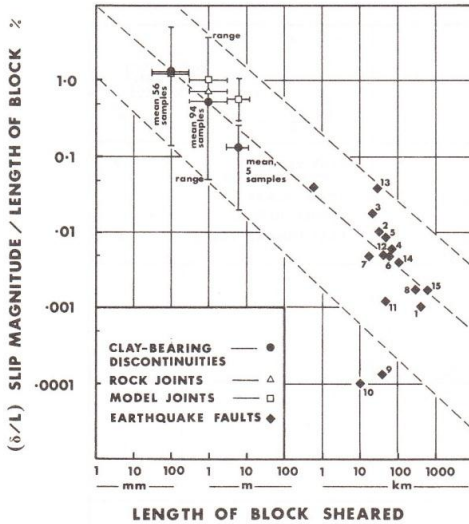


Figure 21. Size-effect exhibited in slip magnitudes. Mean peak displacement data with scatter bars were obtained from Figure 20. Earthquake slip magnitudes were derived from Nur (1974). Number of samples refers to clay-bearing discontinuities only.

8 SCALE EFFECTS ON SHEAR STIFFNESS

Increased block size has been shown to:

increase $\delta(\text{peak})$
 reduce JRC
 reduce JCS

The combined effect is to noticeably reduce the peak shear stiffness (K_S) which was defined to Goodman (1970) as:

$$K_S = \frac{\sigma_h' \tan \phi'}{\delta(\text{peak})} \quad (9)$$

A useful approximation to K_S is given by rearrangement of equations 3, 8 and 9

$$K_S = \frac{\sigma_h' \tan[\text{JRC} \log(\text{JCS}/\sigma_h') + \phi_r]}{\frac{L}{500} \left[\frac{\text{JRC}}{L} \right]^{0.33}} \quad (10)$$

Measured values of K_S derived from a wide ranging review of test data are shown in

Figure 22, each as a function of block size. The stippled lines representing normal stress levels were located using the mean values of JRC, JCS and ϕ_r obtained from the 137 shear tests on rock joints reported by Barton and Choubey (1977):

$$\begin{aligned} \text{JRC} &= 8.9 \\ \text{JCS} &= 92 \text{ MPa} \\ \phi_r &= 27.5^\circ \\ L &= 0.1 \text{ m} \end{aligned}$$

The most frequently measured value of $\delta(\text{peak})$ was 0.6 mm, giving a peak shear stiffness value of 1.7 MPa/mm under a normal stress of 1 MPa. The gradient of the normal stress lines was derived from the best fit relationships (equations 5 and 6) to the data shown in Figure 12.

These equations were derived from shear tests over a ten-fold range of block sizes, and linear extrapolation outside the size range 100 mm - 1 m has been assumed when drawing the effective normal stress diagonals in Figure 22. It will be noted that the earthquake fault stiffnesses (mean values from Nur, 1974) are bracketed by the effective normal stress diagonals 100-1000 MPa (1-10 Kbars).

Tentative application of equations 10, 5 and 6 over a two order of magnitude range of block sizes shown in Figure 23 suggests that there may be a gradual flattening out of the normal stress diagonals with increasing block size. Tentative scaling of the same data to earthquake fault sizes indicates normal stress levels closer to the range 5-20 MPa (50-200 bars). This is conveniently close to the effective normal stress levels operating at depth in the vicinity of the San Andreas fault (Zoback et al. 1980).

Remarkably, equations 5 and 6 also predict near residual (JRC \approx 1.0) surfaces with over-consolidated clay-like properties (JCS \approx 1 to 10 MPa) at fault scale.

It will be noticed that the stiffness of the rough, competent joint and that of the weaker smooth joint (Figure 23) converges when either the stress level, or block size is increased.

The above method of estimating peak shear stiffness for rock joints is specifically directed at clay-free discontinuities. When clay is present, preventing (to a greater or lesser extent) rock-to-rock contact, the peak shear stiffness tends not to be so size-dependent, and is also somewhat less stress dependent, due to the low shear strength (Infanti and Kanji, 1978).

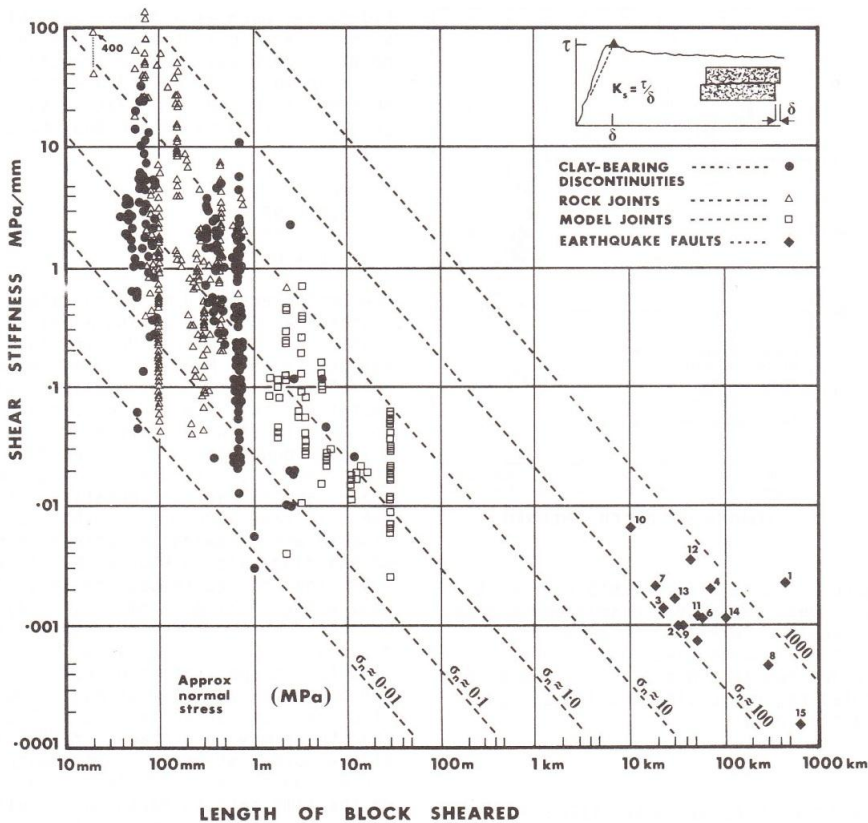


Figure 22. Laboratory and in situ shear stiffness data reported in the literature, indicate the important influence of block size (Barton 1982)

9 CHOOSING APPROPRIATE SHEAR STIFFNESS FOR DESIGN

The choice of appropriate shear stiffnesses in engineering design studies may be critical in decision making. A case in point is the seismic stability of a nuclear power plant foundation, shown schematically in Figure 24.

We can make the immediate assumption that laboratory scale stiffnesses are likely to be meaningless in the stiffness estimation exercise. The next question that arises is whether the natural block sizes (L_0) are large enough. In some cases the answer may be yes. However, the discontinuity structure sketched in Figure 24 has been deliberately designed to include larger blocks (L_1) and those defined by regional scale jointing and by

major bedding planes (L_2). These features are likely to have lower JRC, JCS and ϕ_r values than the smaller block sizes, and may therefore represent the actual division of the foundation into discrete elements.

A numerical experiment, for example using Cundall's (1980) Universal Discrete Element Code (UDEC), could resolve which of the block sizes were most "active" during dynamic motion. The input to such a model would determine the quality of the result. Appropriately scaled values of JRC and JCS for block sizes (L_0) and (L_1), and appropriately chosen values of JRC, JCS and ϕ_r for the major clay-filled features (L_2) would be decisive to the reliability of the modelled behaviour.

Choice, or measurement of the corresponding normal stiffnesses would

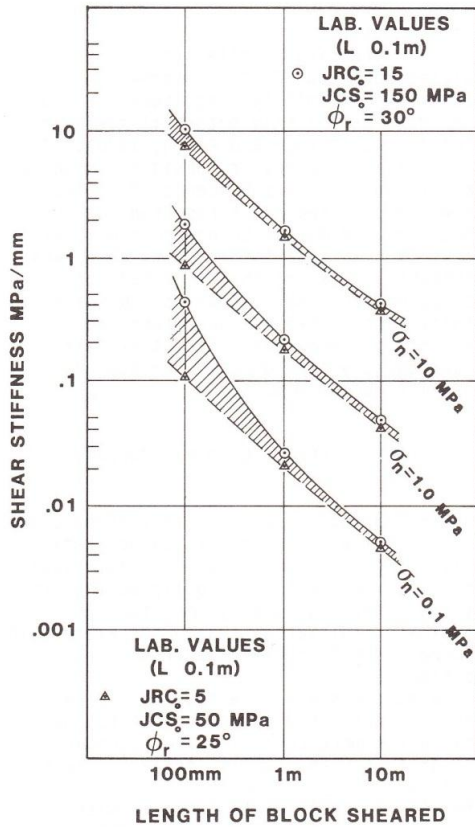


Figure 23. Calculated scale effect on shear stiffness K_S .

present less problem. Normal stiffness is not expected to be scale-dependent along any given discontinuity, but obviously varies considerably from discontinuity to discontinuity, depending on the scale of the given feature; whether it is clay-coated, clay-filled, rough-mating or smooth-mating etc.

An interesting large scale application of low shear stiffnesses in numerical analyses are the UDEC studies of the Ekofisk reservoir subsidence performed by NGI (Barton et al. 1988).

It appeared inherently reasonable to argue that an overburden consisting of 150 km³ of shale with interbeds of limestone, could not behave in practice as a continuum. Bedding planes and sub-vertical or vertical regional joints and faults obviously dissected this huge mass of rock into countless major slabs and blocks, together with the detailed structures that were too numerous to ever consider in any modelling exercise.

When such a body of rock is strained due to an underlying compaction process, deformation occurs by slip rather than bending. Seen in detail, the deformation will resemble the flexure of a leaf spring, with interbed slip due to the stretching required to accommodate the subsidence. Zones of large strains may also cause slip on sub-vertical features, as seen in the more extreme case of long-wall mining.

Since the 150 km³ of overburden had to be modelled with a very small number of blocks, each joint was of fault-like dimensions. Input parameters were chosen using the results of normal and shear loading tests on joints, with extrapolations to fault-sized features (Figures 22, 23).

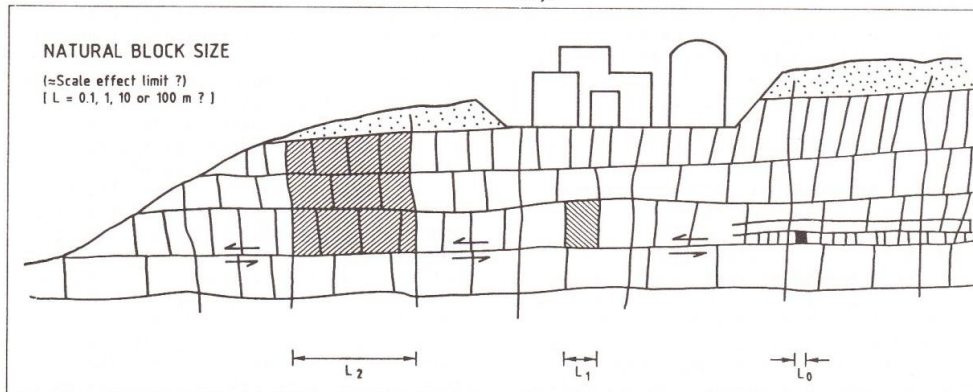


Figure 24. Schematic of nuclear power plant foundation. Choice of appropriate block size for shear stiffness estimation is critical.

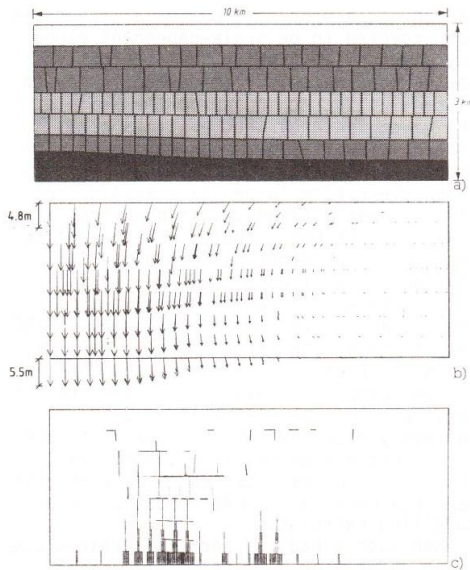


Figure 25. Axisymmetric analyses of reservoir subsidence at Ekofisk using the UDEC method: a) bedding and faults, b) deformation vectors, c) shear displacements.

Initial runs with UDEC, using a linear joint model, and small-scale, high shear stiffnesses, showed continuum type behaviour, with limited slip and characteristically small values of the subsidence-compaction ratio. When shear stiffnesses of the order of 0.01 MPa/mm were used; appropriate to kilometer size faults, behaviour was dominated by bedding plane and fault slip, and ratios of subsidence to compaction were as high as 0.86 to 0.95, which appeared to be consistent with the approximate initial estimates of compaction obtained from logs.

The type of behaviour obtained with realistically low shear stiffnesses is shown in Figure 25. The three diagrams show the assumed geometry, deformation vectors, and zones of joint slip (where line thickness is proportional to slip magnitude).

Maximum values of discontinuity shear were concentrated on vertical and sub-vertical features, the shearing reaching a maximum (for the assumed block size) of 25 cm immediately above the reservoir at a radius of 3 km. The maximum shear on modelled bedding planes was approximately 10 cm, and occurred at the boundary bet-

ween layers of different stiffness at 1600 m depth.

An interesting parallel to this predicted behaviour is the interbedded shear of 23 cm and seismicity (magnitude 2.4 - 3.2) reported at the Wilmington oil field in California (Mayuga and Allen, 1970). In this classic reservoir subsidence problem a maximum surface subsidence of at least 9 m was registered. The reported interbedded shear caused damage to numerous oil well casings. In this instance, movement was concentrated along thin interbeds of claystone and shale sandwiched between thick massive beds of sandstone and siltstone. Numerous wells at Ekofisk have subsequently been damaged, perhaps by similar mechanisms.

10 SCALE EFFECTS CAUSED BY BOUNDARY CONDITIONS

The foregoing example was an extreme case, where choice of input data caused radically different performance in numerical models. However, it is believed that the scale effect is equally important at "normal" engineering scale, for example in tunnel, shaft, rock slope or dam foundation design.

Researchers who have doubted the validity of data showing scale effects, have cited the more complex natural boundary conditions than usually applied in test set-ups. A typical criticism is the failure to test joints in shear with increasing normal stress or normal stiffness control.

Clearly a joint surrounding a tunnel will experience a dilation-related increase in normal stress if it is sheared in this confined environment. It's shear strength may therefore increase with shear displacement. This increase will not of course be seen under a rock slope, or in a shear test conducted under constant normal stress, and shear resistance would in this case gradually decrease following mobilization of the peak shear resistance.

An argument that is occasionally heard is that scale effects on shear strength might not be obtained, if the tests were conducted with normal stiffness control or varying (increasing) normal stress. In fact the opposite is true. Shear tests at different scale conducted with normal stiffness control would experience less increase in normal stress at the larger scale due to reduced dilation. The scale effect would therefore be even more marked than in constant normal stress tests.

11 SCALE EFFECTS IN CONSTITUTIVE STRESS DISPLACEMENT MODELLING

In a companion paper in the Rock Joint Conference; Barton and Bandis (1990) indicate how shear stress - shear displacement curves can be generated for use in discrete element models. The acquisition of input data is also summarized. It is appropriate in the present review paper to concentrate attention on the effect of scale on these and other behaviour modes, for example the dilation and change of joint aperture or conductivity with shear.

We have seen that JRC, JCS and $\delta(\text{peak})$ are each sensitive to the size of joint surfaces or block sizes involved. Equations have been derived to estimate these scale dependencies (refer to equations 5, 6 and 8). We will take

several steps forward and present a joint behaviour model that predicts the onset of dilation with shear under a given normal stress. Numerical models with this dilation subroutine built in will then be capable of tracking the changing normal stress that actually occurs during shear, and continually updating the resulting shear resistance, which is block-size dependent.

Figure 26 illustrates an example of this scale-dependent modelling of shear stress-displacement and dilation-displacement behaviour. The table in the upper figure demonstrates quite marked scale effects on the parameters JRC, JCS and $\delta(\text{peak})$, due to the marked roughness ($JRC_0 = 15$) of the assumed joint. Note the double circles on the three dilation curves, signifying the instant of peak shear resistance. Delayed dilation is also an important feature of the scale effect.

If we consider dilation curve #3, and imagine that it's distance above the axis represents the increased physical aperture (ΔE) of the joint, then we can add this increased aperture to the initial joint aperture E_0 and follow the changing physical aperture ($E_0 + \Delta E$) under shear.

Relating this physical aperture (E) to a conducting aperture (e) must be performed empirically using the relationship shown in Figure 27. This relationship ignores the production of gouge during shear which may tend to block flow channels in softer rocks tested under high stress levels (Makurat et al. 1990a).

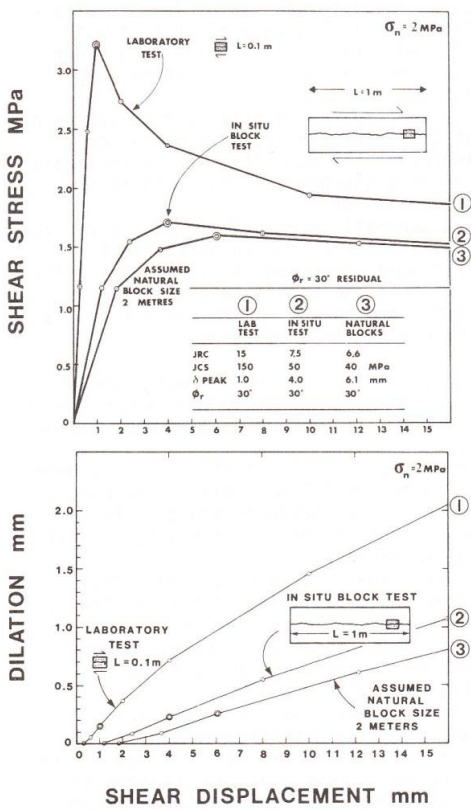


Figure 26. Predicted scale effects on stress-displacement and dilation-displacement behaviour of a rough undulating rock joint (Barton, 1982).

$$e = \frac{(JRC_0)^{2.5}}{(E/e)^2} (\mu\text{m}) \quad (11)$$

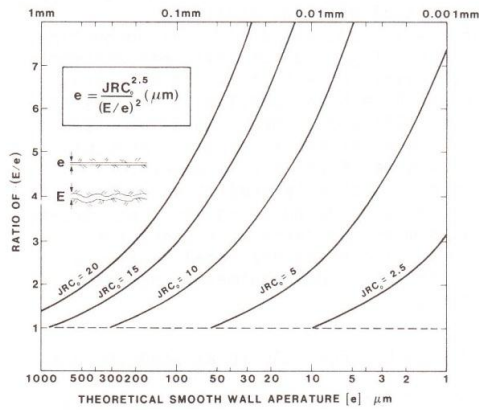


Figure 27. A joint roughness model relating conducting aperture (e) to mechanical aperture (E).

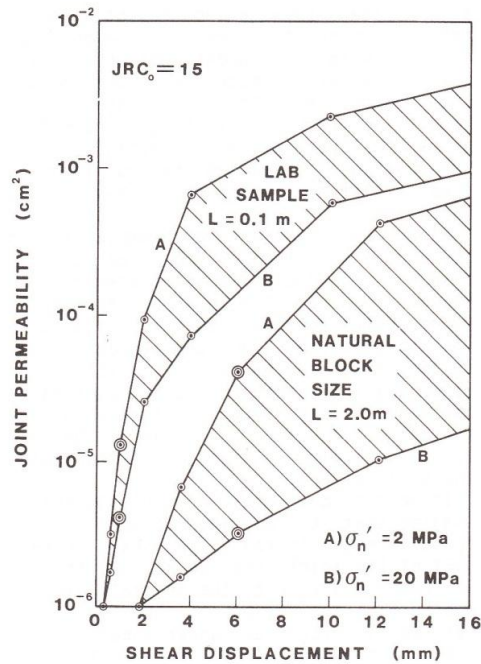


Figure 28. Estimated change in permeability sizes of joint sample when sheared up to, and beyond peak strength (double circles).

The dilation curves #1 and #3 for the 0.1 m and 2.0 m size blocks shown in Figure 26, result in dramatic increases in predicted conductivity with shear, and show correspondingly marked scale effects. Predicted results are shown in Figure 28. An initial physical aperture (E_0) = 174 μm , and an initial conducting aperture (e_0) = 35 μm have been assumed in each case. Note that two normal stress levels have been modelled; 2 MPa (as in Figure 26) and 20 MPa. Gouge produced at the higher stress level would probably block some of the flow channels. The above conductivity predictions must therefore be considered as maxima. Such mechanisms might be favourable under rock slopes (increased drainage), but unfavourable in a dam abutment (increased leakage).

12 SCALE EFFECT CAUSED BY SAMPLING BIAS

NGI is presently involved as one of the Principal Investigators having responsibility for rock mechanics studies in the Stripa Phase III Research programme called

Site Characterization and Validation. Performance of this work during the past two years has made us particularly aware of the fact that sampling bias can cause apparent scale effects. Awareness of these possibilities is obviously important.

Figure 29 illustrates the stages of investigation that have been followed.

The objectives of the rock mechanics programme are as follows:

- to utilize simple joint index testing of numerous joints recovered in drill core to predict the hydromechanical coupled behaviour of joints in the disturbed zone surrounding the validation drift.
- to test the hydromechanical behaviour of selected joints recovered in 200 m cores, using NGI's coupled stress-closure-flow, shear-dilation-flow test (CSFT) (see Makurat et al. 1990b).
- to test the hydromechanical behaviour of an "undisturbed" joint in situ at even larger scale, using a block test with coupled stress-closure-flow, and shear-dilation-flow along the 1400 mm long joint.

- to compare the behaviour of the joints at different scales, as a basis for improving the modelling of the rock mass in the disturbed zone surrounding the validation drift.

A schematic presentation of the various stages of this rock mechanics test programme are given in Figure 29. Joints have been characterized at successively larger scales and in smaller number, as Stage 1 passed into Stage 3.

- Stage 1 174 joints, 100 mm diameter core (NGI)
- Stage 3 5 joints, 200 mm core (NGI, MUN, LULEÅ)
- Stage 3 1 joint, 1000x1000 mm block test (NGI)

Coupled stress-flow tests have also been performed at 200 mm scale in the Memorial University of Newfoundland by John Gale, and at the Technical University of Luleå by Eva Hakami.

The Stage 1 tests have been purely mechanical; utilizing tilt (low stress) shear tests to characterize joint roughness (JRC), and Schmidt hammer rebound testing to characterize joint wall strength (JCS).

Stage 3 tests on the larger joint samples consist of flow testing in combination with mechanical loading. Changes of normal stress ($\Delta\sigma_n$) and changes of shear stress ($\Delta\tau$) cause changes of conducting aperture (Δe) which are of consequence in the final modelling of disturbed zone effects on measured inflows. A sample size effect on all these parameters must be anticipated. The

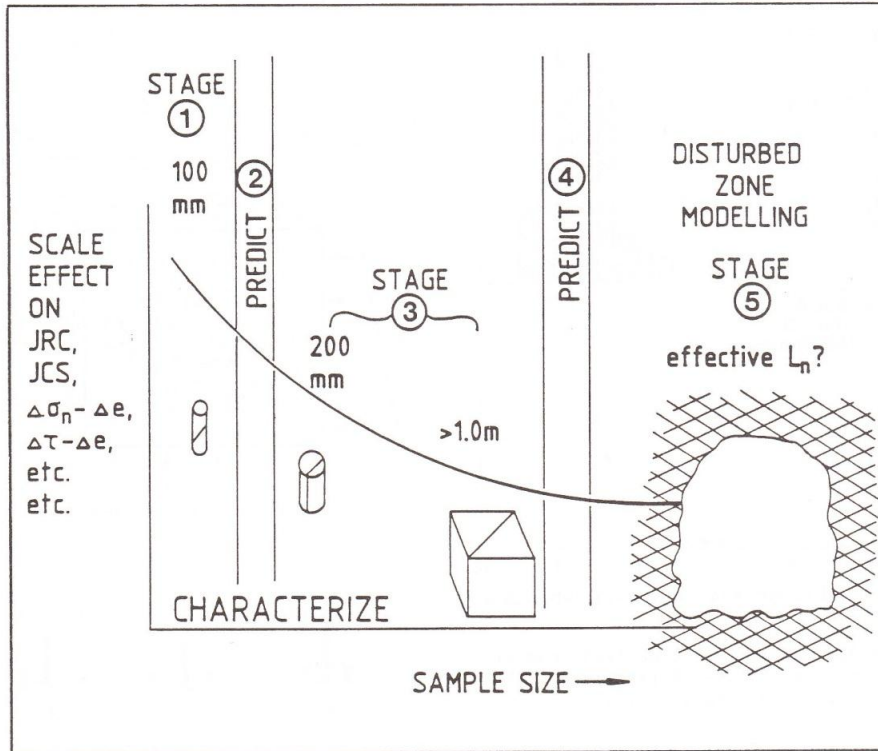


Figure 29. Characterization of joint properties is performed at successively larger scale, in order to predict disturbed zone effects when excavating a tunnel (validation drift).

ultimate scale of testing in Stage 3 is the in situ block test which has been conducted on a jointed block of natural size in the floor of the 3D drift at Stripa.

The joints selected for the coupled CSFT 200 mm lab testing and for the 1400 mm block test, needed to be continuous and reasonably planar, so that problems with stepped surfaces or rock bridges were absent. This choice immediately incorporates a sampling bias, since the most continuous and easily recognized joints at Stripa are rather planar, mineral coated and in many cases actually minor faults.

The CSFT laboratory flow testing was actually conducted on joints with JRC_0 values (200 mm scale) of 1.9 and 3.8. It is immediately clear from the histogram in Figure 30 that they are at the smoothest end of the roughness statistic. The same also applied to the 1400 mm long joint tested in the block test which was the same joint ($JRC_0 = 3.8$) as sampled at 200 mm scale.

Measured stress-flow coupling and shear-dilation-flow coupling is therefore only relevant to the mineral (chlorite) coated minor faults, and bears only moderate resemblance to the expected large scale behaviour of the majority of joints at Stripa.

Set A: Numerous tests at 100 mm scale:
mean: $JRC = 7.1$ $JCS = 120$ MPa $\phi_r = 24.3^\circ$

Set A: Individual CSFT labtests:
 $JRC = 1.9, 3.8$ $JCS = 125$ MPa $\phi_r = 25.1^\circ$

13 SCALE EFFECT STRATEGIES FOR DISCRETE ELEMENT MODELLING

Awareness of the statistical variation of joint properties is essential if the above sampling bias and its effect on measured results is to be correctly incorporated in numerical models. Figure 31 (bottom) illustrates hypothetical statistics for

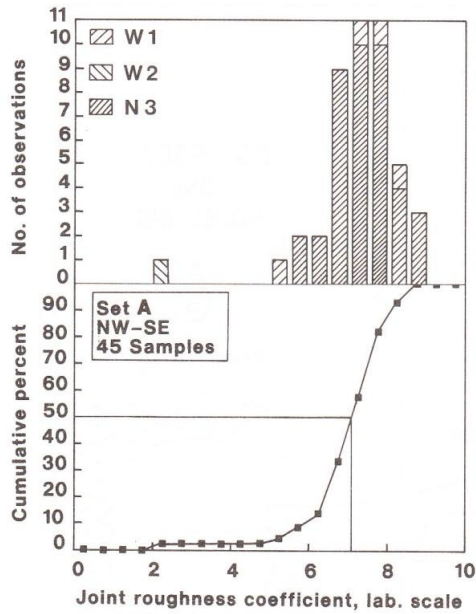


Figure 30. JRC statistic derived from tilt tests on joints of set A (strike NW-SE) at Stripa. Vik and Johansen (1990).

JRC, JCS and ϕ_r for all the joints immediately surrounding a conceptual nuclear waste vault. At the top of the figure an assumed log-normal distribution of joint lengths is given. There are perhaps four numerical modelling strategies for this problem, and only one of them may be more or less equivalent to reality:

- 1 Assume #1 character for all joints (over-conservative)
 - 2 Assume #2 character for all joints (unrealistic)
 - 3 Assume #3 character for all joints (unsafe assumption)
 - 4 Assume length dependent properties (usually correct)
- i.e. character 1111 for longest joints
i.e. character 2222 for average length joints
i.e. character 3333 for shortest joints

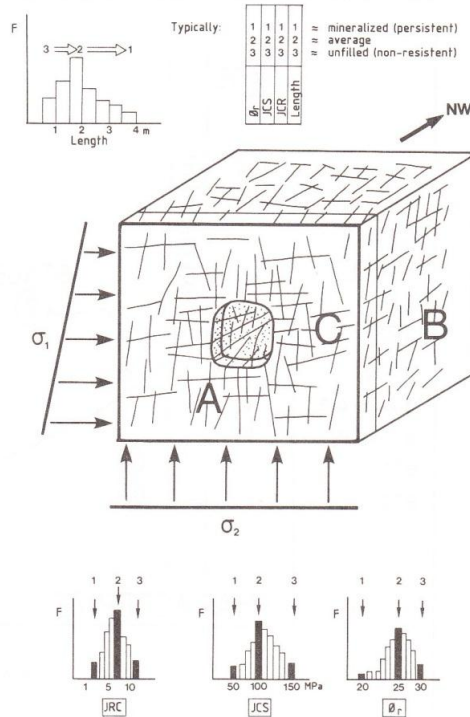


Figure 31. Input data strategy for numerical modelling should consider the length-dependent properties of joints.

Reference to our Rock Joints Conference proceedings (cover photograph) reproduced in Figure 32, will perhaps provide convincing though exaggerated visual evidence that joint length should be considered when assigning mechanical (and hydraulic) properties in a rock mass, or in a discrete element model of the rock mass.

14 SCALE EFFECT INVESTIGATIONS WITH IN SITU STRESS MEASUREMENTS

Great interest in potential scale effects on stress measurements is apparent in this workshop. A most interesting and comprehensive study is reported by Martin et al. (1990) from URL in Canada. These authors have symbolized the range of studies performed in the drawings reproduced in Figure 33.

Although scale effects are implied in the form of presentation, these authors in fact conclude that the chief result of the

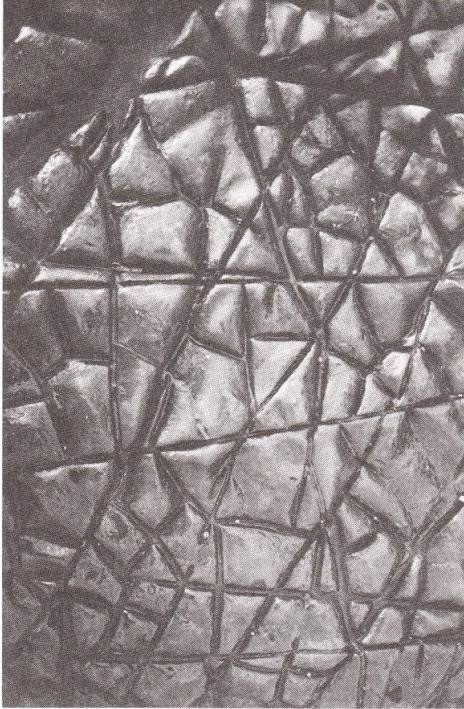


Figure 32. Shorter joints tend to have higher values of JRC, JCS and ϕ_r than more continuous joints.

stress measurement dimension is in the scatter of results. Greatest ranges of measured stress were obtained from the smallest (96 mm) overcores, with successive reduction in measured range at 150 mm. Significantly, the unique 600 mm overcore produced a result almost identical to the mean (Figure 34). No significant scale effect trend beyond this scatter, was identified.

Hydraulic fracturing events produced at different scale in the Camborne Geothermal Energy Research Project were used by Pine et al. (1990, this workshop) to conclude that good quantitative agreement was obtained between methods. They conclude that conventional minifrac, large scale MHF (with water and gel) and microseismic monitoring (of shearing events) give quantitatively consistent results as regards minimum horizontal stress magnitude and principle stress directions.

It is of interest to note the potentially complicating presence of jointing

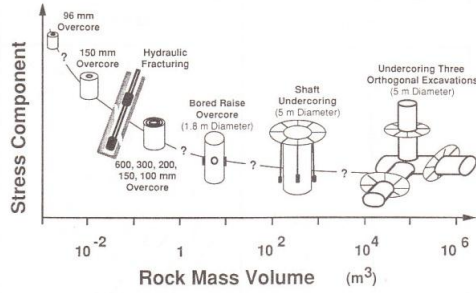


Figure 33. Schematic showing AECL's program to investigate the potential effect of scale on in situ stress measurements (Martin et al. 1990).

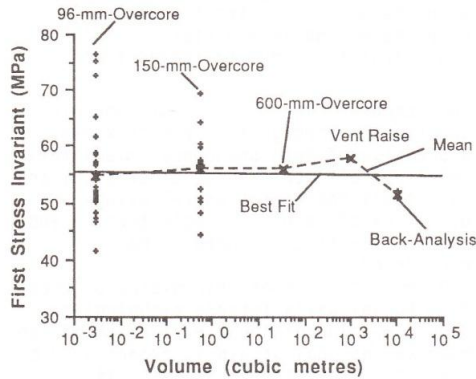


Figure 34. Results of AECL's scale effect investigation. Martin et al. (1990).

in MHF, as shown schematically in Figure 35. To what extent numerical modelling correctly accounts for hydraulically induced shearing events is an interesting exercise in scale effect evaluations, as discussed earlier.

Interesting observations of the influence of wellbore diameter on breakdown pressure in hydraulic fracturing are reported by Ito et al. (1990, this workshop). They produced convincing experimental and theoretical evidence for reduced breakdown pressure with increasing wellbore diameter.

15 SCALE EFFECT FROM EXCAVATION DIMENSION

An obvious extension of the above behaviour from the extensional to the compressional stress regime arises when

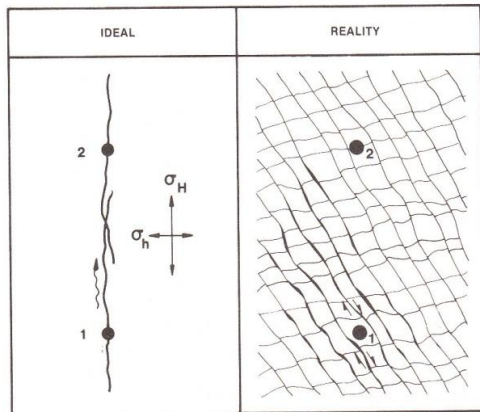
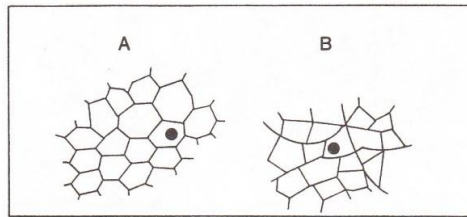


Figure 35. Jointing that is not parallel with the principal stress direction, complicates the interpretation of large scale injection, due to scale effects.

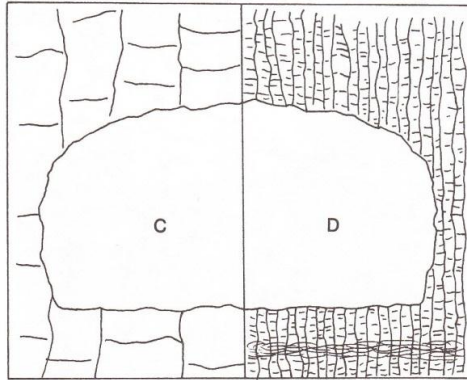
one compares the stability of boreholes and tunnels through the same rockmass. A discussion of such phenomena immediately involves consideration of block size, and the stress-concentration-relieving-qualities of jointing. Both tensile and compressive stresses need to be considered.

Dynamic release of thin plates of rock from tunnel walls (stress slabbing) may occur in an underground excavation if too much extensional strain is experienced by the rock in question. However, if jointing is present, extensional strain and shear strain can be accommodated more readily and are partially dissipated. Paradoxically, the excavation of an underground opening in a highly stressed environment is likely to be less hazardous when the rock is jointed than when it is intact. This is a form of scale effect caused by joint spacing or block size.

Stress levels at 900 m depth in basalt at the Hanford Site (previously nominated for USA's nuclear waste disposal) indicated high levels of differential stress ($\sigma_H/\sigma_V = 2.3-2.7$) which caused extensive core discing in the relevant 900-1000 m depth, and extensively damaged ("dog eared") borehole walls, with increased dimensions across their E-W diameters, perpendicular to the σ_H direction. This observation in boreholes and drillcore caused obvious concern when considering the performance of shafts and repository tunnels at equivalent depths. It was estimated at the time that when thermal loading is superimposed on the virgin



(a) Boreholes in "massive" rock.



(b) Tunnels in jointed rock.

Figure 36. Large relative block sizes experienced by boreholes A and B cause borehole wall failure ("dog-earing"). Tunnels driven in the same highly stressed rock might suffer stress slabbing in case C, but not in case D, owing to the strain relieving nature of the joints.

stress field, due to the highly radioactive waste, the effective value of σ_H may be as high as 100 MPa locally, resulting in stress concentrations as high as 150 MPa round the elliptical tunnels.

Application of the tunnel reinforcement guidelines in the Q system (Barton, 1987) to this problem suggested that mild rock bursting or stress slabbing might occur in the massive colonnade section of the basalt flow with its characteristic hexagonal columns, but was unlikely in the more heavily jointed entablature. The occurrence of "dog-earing" in excavations of borehole size may will be due to the relative scarcity of strain relieving joints at this scale. As suggested in Figure 36, the problem is dependent on relative block size which can be defined as the ratio of the excavation span and the average block size.

Physical model studies reported by Barton & Hansteen (1979) provide some support for this hypothesis. Model tunnels were excavated in highly anisotropic stress fields. In most of the excavations, the smallest top headings had a relative block size of 1/12, i.e. 12 blocks per span width. In no cases were blocks fractured by the highly anisotropic stress. Tunnel deformation was marked (0.5% of span) and was caused mainly by extensional strain relief and shear on the joints.

A model with particularly large joint spacing was specially constructed to facilitate simulation, using a jointed finite element code. The model contained only 1200 discrete blocks instead of the usual 20 000 blocks. It had the same extreme stress distribution, the same joint orientations and the same excavation methods were used. Deformation around the opening was greatly reduced, and stress slabbing was observed. The relative block size was in this case 1/2. Jointing can be advantageous when excavating in high stress fields, and is clearly responsible for a block size scale effect.

The effects caused by increasing the dimensions of the top heading of a rock cavern to the full cross-section either in physical models, FEM, UDEC, or in practice, are obvious, and should perhaps not be included in a discussion on scale effects. Nevertheless, some interesting comments on scale effects that extend the above discussion to underground excavations in general are made by Fukushima (1990, this workshop).

CONCLUSIONS

1. Scale effects have been identified in numerous processes of concern to rock mechanics engineers. Nevertheless, the scale effect that may be induced by the sampling process should never be underestimated. Larger samples are more difficult to gain access to, they are more difficult to prepare, and the result of all these preparatory steps may result in an exaggerated observation of the actual scale effect, which might have been minor.

2. Scale effects on compression strength and on deformability in general, appear to be inevitable due to the "flawed" and jointed nature of rocks and rock masses respectively. A wealth of data is available to support this widely accepted view.

3. Scale effects are particularly well documented for joint behaviour in shear. Fundamental geometrical scale effects are

evident when sampling (i) angles at different scale. These are evident in the joint roughness coefficient (JRC) scale effect. Since asperities may fail in shear, the size of asperity that is loaded may cause an additional compression or tensile strength scale effect. This can be accounted for by scale correction factors for the joint compression strength (JCS) parameter.

4. The shear displacement required to mobilize peak strength is also scale dependent, increasing with larger joint samples or with larger block sizes. For this reason the shear stiffness of a joint may be doubly scale dependent.

5. The statistical variation of joint parameters within one joint set, and within the rock mass as a whole, should be carefully considered when selecting samples for special tests, for example in situ block tests. Due to the expense of the special test, there may be a temptation to assume that the results obtained are generally applicable. The special test may in fact have been performed on an "extreme value" discontinuity, due to the ease of recognition and areal extent of such features.

6. Investigations of potential scale effects on stress measurements by over-coring appear to show larger scatter at small scale, but otherwise no significant trends in terms of mean magnitudes. Evaluation of scale effects in hydraulic fracturing appear to show scale effects on breakdown pressure, but not for minimum principal stress or stress orientations. The complicating influence of joint shearing may need special consideration here, due to the scale dependence of shear-dilation-conductivity coupling.

7. Block size appears to be an extremely important parameter for explaining a wide range of scale effects in rock engineering including compression strength, deformation modulus, shear strength, dilation, conductivity, shear stiffness, failure mode, stress-strain behaviour, tunnel closure, reinforcement requirements, etc.

REFERENCES

- Bakhtar, K. and N. Barton 1984. Large Scale Static and Dynamic Friction Experiments, Proc. 25th US Rock Mechanics Symp. Northeastern Univ. Illinois.
- Bandis, S., A. Lumsden and N. Barton, 1981. Experimental studies of scale effects on the shear behaviour of rock joints, Int. J. of Rock Mech. Min. Sci. and Geomech. Abstr. 18, pp. 1-21.

- Bandis, S., A.C. Lumsden and N. Barton 1983. Fundamentals of Rock Joint Deformation. *Int. J. Rock Mech. Min. Sci. and Geomech. Abstr.* Vol 20, No. 6, pp. 249-268.
- Barton, N. 1971. A relationship between joint roughness and joint shear strength. *Proc. of Symp. of Int. Soc. Rock Mech. Rock Fracture, Nancy*, paper I.8, 20 pp.
- Barton, N. 1976. The shear strength of rock and rock joints. *Int. Jour. Rock Mech. Min. Sci. and Geomech. Abstr.*, Vol. 13, No. 9, pp. 255-279. Also NGI-Publ. 119, 1978.
- Barton, N. and V. Choubey 1977. The shear strength of rock joints in theory and practice, *Rock Mechanics*, Springer, Vienna, No. 1/2, pp- 1-54. Also NGI-Publ. 119, 1978.
- Barton, N. and H. Hansteen 1979. Very large span openings at shallow depth: Deformation magnitudes from jointed models and F.E. analysis. *Proc. 4th Rapid Excavation and Tunneling Conference. Atlanta, Ch. 77*, pp. 1331-1353.
- Barton, N. 1980. Estimation of in situ joint properties, N asliden mine, *Int. Conf. on Application of Rock Mechanics to Cut-and-Fill Mining*, Lule , Sweden, Institution of Mining and Metallurgy, London.
- Barton, N. 1982. Modelling rock joint behavior from in situ block tests: Implications for nuclear waste repository design, *Office of Nuclear Waste Isolation, Columbus, OH*, 96 p., ONWI-308, September 1982.
- Barton, N. and S. Bandis 1982. Effects of Block Size on the Shear Behavior of Jointed Rock, *Keynote Lecture, 23rd U.S. Symposium on Rock Mechanics*, Berkeley, California.
- Barton, N. 1986. Deformation Phenomena in Jointed Rock. 8th Laurits Bjerrum Memorial Lecture, Oslo. *Publ. in Geotechnique, Vol. 36, No. 2*, pp. 147-167.
- Barton, N. 1987. Rock Mass Classification and Tunnel Reinforcement Selection using the Q-system. *Proc. ASTM Symp. on Rock Classification Systems for Engineering Purposes*, Cincinnati, Ohio
- Barton, N. and S. Bandis 1990. Review of predictive capabilities of JRC-JCS model in engineering practice. *Proc. ISRM conf. on Rock Joints*, Loen, Norway, Balkema Press.
- Byerlee, J.D. 1978. Friction in Rocks. *Journal of Pure and Applied Geophysics*, Vol. 116, pp.615-626.
- Cundall, P.A. 1980. A generalized distinct element program for modelling jointed rock. Report PCAR-1-80, Contract DAJA37-79-C-0548, European Research Office, US Army, Peter Cundall Associates.
- Fecker, E. and N. Rengers 1971. Measurement of large scale roughness of rock planes by means of profilograph and geological compass. *Proc. Int. symp. on Rock Fracture, Nancy (ISRM) Paper 1-18*.
- Fukushima, K. 1990. Scale effects on the underground excavation. *Proc. of 1st. Int. Workshop on Scale Effects in Rock Masses*, Loen, Norway, Balkema Press.
- Goodman, R.E. 1970. Determination of the in-situ modulus of deformation of rock. *Deformability of Joints Symposium, American Society for Testing Materials, S.T.P. 477*, pp 174-196.
- Hoek, E. and E.T. Brown 1980. *Underground excavations in rock*. Institution of Mining and Metallurgy, 527 p.
- Hencher, S.R. and L.R. Richards 1982. The basic frictional resistance of sheeting joints in Hong Kong granite. *Hong Kong Engineer*, Feb. 82, pp. 21-25.
- Hencher, S.R. and L.R. Richards 1989. Laboratory direct shear testing of rock discontinuities. *Ground Engineering*, March 89, pp.24-31.
- Infanti, n. and M.A. Kanji 1978. In-situ shear strength, normal and shear stiffness determinations at Agua Vermelha Project. *Proc. of 3rd Intl. Cong. of the Intl. Assn. of Engineering Geologists*, held in Madrid, Spain, Session 2, Vol. 2, pp. 175-183.
- Ito, T., K. Hayashi and H. Ab  1990. Scale effects in breakdown pressures of hydraulic fracturing stress measurements. *Proc. of 1st Int. Workshop on Scale Effects in Rock Masses*, Loen, Norway, Balkema Press.
- Jackson, R. and J.S.O. Lau 1990. The effect of specimen size on the mechanical properties of Lac du Bonnet grey granite.
- Lama, R.D. and L.P. Gonano 1976. Size-effect considerations in the assessment of mechanical properties of rock masses. *In: Proceedings of the Second Symposium on Rock Mechanics*, Dhanbad.
- Maertz, N.H. and J.A. Franklin 1990. Roughness scale effect and fractal dimension. *Proc. of 1st Int. Workshop on Scale Effects in Rock Masses*, Loen, Norway, Balkema Press.
- Mayuga, M.N. and D.R. Allen 1970. Subsidence in the Wilmington oil field, Long Beach, California, USA. *Proc. UNESCO Conf. on Land Subsidence*, Vol. 1, pp.66-79.
- Makurat, A., N. Barton, N.S. Rad and S. Bandis 1990. Joint conductivity variation due to normal and shear defor-

- mation. Proc. of ISRM Conf. on Rock Joints, Loen, Norway.
- Makurat, A., N. Barton, L. Tunbridge and G. Vik 1990. The measurement of the mechanical and hydraulic properties of rock joints at different scales in the Stripa project. Proc. of ISRM Conf. on Rock Joints, Loen, Norway.
- Martin, C.D., R.S. Read and N.A. Chandler 1990. Does scale influence in situ stress measurements? - Some findings at the Underground Research Laboratory. Proc. of 1st Int. Workshop on Scale Effects in Rock Masses, Loen, Norway, Balkema Press.
- Nur, A. 1974. Tectonophysics: The study of relations between deformation and forces in the earth. Proc. of the 3rd Intl. Cong. on Rock Mech., held in Denver, CO, Vol. 1A, pp 243-317.
- Patton, F.D. 1966. Multiple modes of shear failure in rock. Proc. 1st Cong. Int. Soc. Rock Mech., Lisbon, 1: 509-513.
- Pine, R.J., L.W. Tunbridge and A. Jupe 1990. An evaluation of in situ stress measurements affecting different volumes of rock in the Carnmenellis granite. Proc. of 1st Int. Workshop on Scale Effects in Rock Masses, Loen, Norway, Balkema Press.
- Richards, L.R. and J.W. Cowland 1982. The effect of surface roughness on the field shear strength of sheeting joints in Hong Kong granite. Hong Kong Engineer, Oct. 82, pp. 39-43.
- Vik, G. and P.M. Johansen 1990. Determination of shear strength of rock joints at two dam sites and at Stripa Research Mine. Proc. of ISRM Conf. on Rock Joints, Loen, Norway.
- Wagner, H. 1987. Design and support of underground excavations in highly stressed rock. Keynote paper, Proc. of 6th ISRM Congress, Montreal (Vol. 3, reprint by courtesy of author).
- Zoback, M.D., H. Tsukahara and S. Hickman 1980. Stress measurements at depth in the Vicinity of the San Andreas Fault: Implications for the magnitude of shear stress with depth. J. Geophys. Res., Vol. 85, pp. 6157-6173.